Life Sciences 232 (2019) 116654

Contents lists available at ScienceDirect

Life Sciences

journal homepage: www.elsevier.com/locate/lifescie

Ghrelin improves muscle function in dystrophin-deficient *mdx* mice by inhibiting NLRP3 inflammasome activation

Leilei Chang[a,b], Fengnan Niu[c], Jian Chen[a], Xiang Cao[b], Zhuo Liu[b], Xinyu Bao[b], Yun Xu[a,b,*]

[a] Department of Neurology, Nanjing Drum Tower Hospital Clinical College of Nanjing Medical University, Nanjing 210008, Jiangsu, China
[b] Department of Neurology, Affiliated Drum Tower Hospital, Jiangsu Key Laboratory for Molecular Medicine, Nanjing University Medical School, Nanjing 210008, Jiangsu, China
[c] Department of Pathology, Affiliated Drum Tower Hospital, Nanjing University Medical School, Nanjing 210008, Jiangsu, China

ARTICLE INFO

Keywords:
Duchenne muscular dystrophy
mdx
Ghrelin
NLRP3 inflammasome
IL-1β
Muscle function

ABSTRACT

Aims: Immuno-inflammation contributes to the pathogenesis of Duchenne muscular dystrophy (DMD), characterized by progressive muscle degeneration and weakness. The nucleotide-binding oligomerization domain (NOD)-like receptor family pyrin domain containing 3 (NLRP3) inflammasome is crucial for initiating innate immunity. Ghrelin is a circulating hormone that exerts anti-inflammatory activity in several inflammatory diseases. However, the role of ghrelin in DMD and underlying mechanism are still unstated. Therefore, we investigated the effect and potential mechanism of ghrelin on muscle morphology and muscular function of *mdx* mice, a mouse model of DMD.

Main methods: 4-Week-old male *mdx* mice were injected intraperitoneally with ghrelin (100 μg/kg of body weight/day) or saline for 4 weeks. Then, muscle performance was evaluated by behavioral tests. Skeletal muscles samples were collected and relevant parameters were measured by using histopathological analysis and molecular biology techniques both in *mdx* muscles and primary myoblasts.

Key findings: Ghrelin significantly improved motor performance, alleviated muscle pathology and decreased inflammatory cell infiltration in *mdx* mice. Importantly, ghrelin dramatically inhibited NLRP3 inflammasome activation and reduced the production of mature IL-1β both in dystrophic muscles and in lipopolysaccharide (LPS)-primed primary myoblasts induced by the NLRP3 inflammasome activator benzylated ATP (BzATP). Furthermore, the inhibition of NLRP3 inflammasome by ghrelin was partly mediated by the suppression of JAK2-STAT3 and p38 MAPK signaling pathway.

Significance: Our findings reveal that ghrelin suppresses muscle inflammation and ameliorates disease phenotype through inhibition of NLRP3 inflammasome activation and the production of IL-1β in *mdx* mice, which suggests new therapeutic potential of ghrelin in DMD.

1. Introduction

Duchenne muscular dystrophy (DMD) is a severe genetic muscle disease attributed to mutations in the dystrophin gene, presenting progressive muscle weakness, loss of ability to walk and death at the age of 20–30s [1]. The mdx mouse model, as the most widely used animal model of DMD, shows a similar skeletal muscle pathology to DMD patients at 3 to 8 weeks of age [2]. In 2016, the US Food and Drug Administration (FDA) approved Eteplirsen, an antisense oligomer that triggers exon skipping, which is applicable for nearly 14% of patients with *DMD* mutations. It has been generally recognized that multiple immune cells and pro-inflammatory cytokines infiltrated in dystrophic skeletal muscles exacerbate muscle damage in *mdx* mice [3,4]. Rising evidence shows that the immune response plays a central role in pathogenesis of DMD. Reducing inflammation via a variety of interventions ameliorates muscle phenotype and muscle function [5–8]. Presently, glucocorticoids are the accepted therapeutic approach owing to their anti-inflammatory effects; however their short-term benefits are accompanied by considerable side effects, such as hyperglycemia, hypertension and osteoporosis [9]. Therefore, it is urgent to identify alternative therapies for regulating the immune response and slowing down disease progression in DMD patients.

Ghrelin as a peptide hormone chiefly produced by the stomach, plays significant roles in regulating appetite, growth hormone release

* Corresponding author at: Department of Neurology, Nanjing Drum Tower Hospital, Clinical College of Nanjing Medical University, 321 ZhongShan Road, Nanjing City, Jiangsu Province 210008, China.
E-mail address: xuyun20042001@aliyun.com (Y. Xu).

https://doi.org/10.1016/j.lfs.2019.116654
Received 18 February 2019; Received in revised form 11 July 2019; Accepted 11 July 2019
Available online 12 July 2019

and energy balance through binding to its receptor growth hormone secretagogue receptor-1a (GHSR-1a) [10–12]. It has been reported that ghrelin exerts anti-inflammatory effects in several inflammatory diseases, such as hepatic, kidney diseases and cardiovascular diseases [13–15]. Meanwhile, ghrelin binding in cardiac tissue is altered with cardiovascular inflammation in DMD [16]. In addition, previous studies have demonstrated that ghrelin prevents skeletal muscle atrophy and promotes myoblast differentiation in a GHSR-1a–independent manner [11,17]. Furthermore, Reano et al. [12] have illustrated that unacylated ghrelin enhances muscle regeneration, improves dystrophic phenotype and muscle function in *mdx* mice. However, the effect of ghrelin in DMD and the potential mechanism, especially inflammatory response, is largely unknown and needs to be explored.

The Nucleotide-binding oligomerization domain-like receptor protein 3 (NLRP3) inflammasome is responsible for initiating sterile inflammatory responses to tissue injury [18]. It is composed of NLRP3, apoptosis-associated speck-like protein containing a caspase recruitment domain (ASC) and caspase-1. The NLRP3 inflammasome as a cytoplasmic multiprotein complex mediates maturation and secretion of the cytokines interleukin 1β (IL-1β) and IL-18 to trigger the innate immune response, which is activated by endogenous and exogenous molecules such as ATP, cell debris, pathogenic microbes [19,20]. Also, it has been established that the NLRP3 inflammasome plays an important role in metabolic and autoimmune diseases [21]. Remarkably, Raphaël et al. have found that the NLRP3 inflammasome is activated in skeletal muscle and contribute to muscle inflammation in DMD patients and *mdx* mice [22]. Therefore, recognition of potential interventions for inhibiting the NLRP3 inflammasome activation and associated mechanisms may provide a new therapeutic strategy for DMD. In the present study, we aimed to explore the potential effects of ghrelin on motor performance and muscular pathology in dystrophic muscles and further investigate the underling mechanisms by using the *mdx* mouse model of DMD and primary myoblasts.

2. Materials and methods

2.1. Animals

The animal study protocols were approved by the Committee of Experimental Animal Administration of Nanjing Medical University and operated according to the guidelines for Laboratory Animal Care and Use provided by the National Institutes of Health.

Male C57BL/10ScSn-Dmd*mdx*/NJU (*mdx*) mice (aged 4 weeks, weighing 10–18 g) were purchased from Nanjing Biomedical Research Institute of Nanjing University. Four weeks old male wild-type C57BL/10 mice (WT) provided by the Animal Center of Drum Tower Hospital, were also used in the present study. Mice were housed in a controlled conditions room with a 12-hour light/dark cycle and obtained standard mouse chow and water ad libitum.

Animals were randomly divided into four groups: saline-treated and ghrelin-treated wild-type C57BL/10 mice (WT), saline-treated *mdx* mice and ghrelin-treated *mdx* mice. In ghrelin-treated *mdx* mice group, 4-week-old male *mdx* mice received an intraperitoneal (IP) injection of ghrelin (100 μg/kg of body weight/day) for 4 weeks. Saline was used as a control in the other two groups. After 4 weeks injection, all animals were subjected to muscle strength measurement and wire test after above interventions. Then, the animals were euthanized and skeletal muscle tissues (quadriceps, tibialis anterior and gastrocnemius muscles) from three groups were collected and frozen in liquid nitrogen for the following experiments.

2.2. NLRP3- lentivirus injection

Our study used short hairpin RNA (shRNA) to knockdown muscular NLRP3 expression. The scrambled shRNA plasmids were used as negative controls. The sequences of NLRP3 shRNA and scrambled shRNA were as follows: shRNA1 sequence:sense:5′-ACATGACTTTCCAGGAGTT-3′,anti-sense:5′-AACTCCTGGAAAGTCATGTGG-3′;shRNA2 sequence: sense: 5′- GGATTGAAGTGAAAGCCAA-3′, anti-sense:5′-TTGGCTTTCACTTCAATCCAC-3′;shRNA3sequence:sense:5′-CGGACTGTAAACTACAGAT-3′, anti-sense: 5′- ATCTGTAGTTTACAGTCCGGG-3′; scrambled shRNA sequence: sense: 5′-UUCUCCGAACGUGUCACGUTT-3′, anti-sense: 5′-ACGUGACACGUUCGGAGAATT-3′. NLRP3-specific shRNA (GeneChem, Shanghai, China) or control scrambled shRNA (GeneChem, shanghai, China) were delivered by three separate intramuscular injections into skeletal muscles of 4-week-old *mdx* mice using a stereotaxic apparatus as described previously [23]. Then, muscle function was performed at 4 weeks after the lentivirus injection, and muscle tissues were isolated for other experiments as described below.

2.3. Grip strength test

As previously described [24], muscle strength of mice forelimbs was measured by a computerized grip strength meter apparatus (Model 47,200, UGO Basile, Italy), which consists of a peak amplifier and a grasping trapeze attached to a force transducer. The animal is placed to grasp the trapeze. Using one hand, the operator grasps the base of the tail and pulls it steadily (about 2 cm/s) until the grip is broken. The peak pulling force (grip strength) was recorded. Five measurements are taken for each animal, with an intertrial interval of 1 min. The grip strength is normalized by body weight and the results are expressed as mean values of grip strength.

2.4. Wire suspension

This test measures an animal's ability to grasp a horizontal wire with its forepaws and to remain suspended [24]. In this test, a metal wire (diameter 1.5 mm) was suspended between two wooden platforms and was elevated to a height of 20 cm above a cushion, which protected the animals form injury during falls. The longest time for which the mouse is able to cling onto the horizontal string and the drop times with 3 min are recorded.

2.5. Histological analysis

Skeletal muscle tissues were removed and fixed in precooled isopentane with liquid nitrogen. Then, cross-sections from frozen muscle tissues were cut on a standard cryostat with a clean blade. According to standard protocols, frozen sections were stained with hematoxylin and eosin (H&E). Images were photographed and recorded by using a Nikon TE200 microscope with a Spot RT digital camera. Morphometric analysis of muscle fibers was performed using ImageJ software, including the percentage of centrally nucleated fibers and the minimum Feret's diameter of myofibers. We also evaluated the variance coefficient of muscle fiber size using the following formula: variance coefficient = (standard deviation of the muscle fiber size/ mean muscle fiber size) × 1000 as previously published [5]. Above analysis was performed on 500 muscle fibers from five squares randomly chosen on each H&E cross-section [5]. In addition, the proportion of different sizes of muscle fibers in total number of myofibers was calculated for quanfication of fiber size distribution (150–200 muscle fibers/image, 5 images/mouse, 3 mice/genotype).

2.6. Immunohistochemistry and immunofluorescence

According to previously published techniques [5,25], muscle sections from all above groups were rinsed three times with phosphate buffered saline (PBS), permeabilized with PBS/0.1% Triton-X100 for 30 min at room temperature. Then, muscle sections were blocked with 2% bovine serum albumin (BSA) in PBS with 0.05% Triton-X100 (PBST) for 2 h at room temperature and subsequently incubated with CD8 or

F4/80 (1:500, Abcam, Cambridge, UK) overnight at 4 °C. The sections were washed three times with PBS and then incubated with secondary antibodies for 2 h at room temperature. For F4/80 immunofluorescence staining, an Alexa Fluor® 594-conjugated Donkey anti-rat IgG polyclonal (1/200) was used as the secondary antibody. After additional three washes with PBS, images were captured by using a Nikon TE200 microscope. The results for positive-stained area were then presented as a percentage of the total muscle sections area, which were quantified by using ImageJ software. Moreover, the quantification was at least from three independent experiments in a randomized and blinded manner.

2.7. Primary myoblast isolation and culture

Primary myoblasts were separated from the hind limb muscles of 8-day-old *mdx* mice as reported elsewhere [26]. Briefly, muscle tissues were cut into small pieces and digested in an enzyme mix containing 0.2% collagenase type-I and 0.125% trypsin in Dulbecco's modified Eagle's medium (DMEM; Invitrogen, USA) for 1 h at 37 °C. The digested tissues were then transferred into DMEM supplemented with 10% fetal bovine serum (FBS), passed through a serological pipette, filtered through a 40 μm cell strainer and centrifuged at 300 ×*g* for 10 min. The cell pellet was further resuspended in DMEM containing 20% FBS, 0.5% chick embryo extract, 1% penicillin/streptomycin and 2 mmol/L L-glutamine. For removing fibroblasts, muscle cells were then plated on non-coated culture dishes in a 37 °C/5% CO_2 incubator for 1 h. After that, cells were cultured on collagen-coated plates in above growth medium for 10 days and then used in the following experiments.

Activation of NLRP3 inflammasome

To assess the effect of ghrelin on NLRP3 inflammasome activation [26,27], primary myoblasts were seeded in 6-well plates for 2 days. The cells were then primed with lipopolysaccharide (LPS, 1 μg/mL) for 5 h, incubated with ghrelin (100 nM) for 1 h and sequentially stimulated with the P2X7 receptor agonist benzylated ATP (BzATP; Sigma-Aldrich) at 5 mM for 30 min. Finally, the supernatants and cell lysates were collected and analyzed for NLRP3 inflammasome component by western blotting and for IL-1β production by enzyme-linked immunosorbent assay (ELISA).

2.8. RNA isolation and quantitative real-time PCR

According to the manufacturer's instructions, total RNA was extracted from muscle tissues via TRIzol reagent (Invitrogen, Carlsbad, CA, USA) and reverse-transcribed into cDNA using a PrimeScript RT reagent kit (Takara, Dalian, China). Quantitative real-time PCR (qRT-PCR) was performed on ABI 7500 instrument (Applied Biosystems, USA) with a fluorescent dye (SYBR GreenI; Takara) as previously reported protocol [23]. The relative quantification of mRNA level was analyzed after normalized to GAPDH mRNA using the comparative cycle threshold (Ct) method. Each sample was examined in triplicate. Primer sequences (Invitrogen, Frederick, MD, USA) are as follow:

NLRP3 Forward: GTGGAGATCCTAGGTTTCTCTG,
NLRP3 Reverse: CAGGATCTCATTCTCTTGGATC;
ASC Forward: GGAGTCGTATGGCTTGGAGC,
ASC Reverse: CGTCCACTTCTGTGACCCTG;
Capase-1 Forward: AGGCACGGGACCTATGTGAT,
Capase-1 Reverse: AGGGCAAAACTTGAGGGTCC;
IL-1β Forward: AAGCCTCGTGCTGTCGGACC,
IL-1β Reverse: TGAGGCCCAAGGCCACAGG;
β-Actin Forward: GGCCAACCGTGAAAAGATGA,
β-Actin Reverse: GACCAGAGGCATACAGGGACAA.

2.9. Western blot analysis

Western blot analysis was carried out as previously described [28]. First, proteins from the muscle tissues were separated by RIPA lysis buffer (Thermo Scientific, USA), and the protein concentrations were determined using a BCA protein assay kit (Thermo Scientific, USA) in accordance with the manufacturer's instructions. Next, equal amounts of total protein samples were isolated by 10% sodium dodecyl sulphate-polyacrylamide gel electrophoresis (SDS-PAGE) and transferred onto PVDF membranes (Millipore, USA).The membranes were blocked with 5% non-fat milk for 1 h at room temperature and then incubated with the following primary antibody overnight at 4 °C: anti-NLRP3 (1:1000, Cell Signaling Technology, USA; cat. no. 15101), anti-ASC (1:1000, Cell Signaling Technology, USA; cat. no. 67824), anti-caspase-1 (1:1000, Abcam, USA; cat. no. ab1872), anti-cleaved caspase-1(p20) (1:500, AdipoGen, USA; cat. no. AG-20B-0042), anti-IL-1β (1:1000, Cell Signaling Technology, USA; cat. no. 12242), anti-JAK2 (D2E12) (1:1000, Cell Signaling Technology, USA; cat. no. 3230), anti-p-JAK2 (Tyr1007/1008) (1:1000, Cell Signaling Technology, USA; cat. no. 3771), anti-STAT3 (79D7) (1:1000, Cell Signaling Technology, USA; cat. no. 4904), anti-p-STAT3 (Tyr705) (1:1000, Cell Signaling Technology, USA; cat. no. 9131), anti-JNK (1:1000, Cell Signaling Technology, USA; cat. no. 9252), anti-p-JNK (Thr183/Tyr185) (1:1000, Cell Signaling Technology, USA; cat. no. 4668), anti-p38 MAPK (D13E1) (1:1000, Cell Signaling Technology, USA; cat. no. 8690), anti-p-p38 MAPK (Thr180/Tyr182) (1:1000, Cell Signaling Technology, USA; cat. no. 4511), followed by HRP-conjugated anti-rabbit or anti-mouse secondary antibodies (1:5000, BioWorld, USA) for 2 h at room temperature. The blots were determined using a Chemiluminescence ECL kit (Thermo Scientific, USA). The intensity of bands was quantified using Image J software. Anti-GAPDH (1: 5000, BioWorld, USA, Cat. No. MB9231) was used as a loading control. All experiments were performed at least in triplicate.

2.10. Enzyme-linked immunosorbent assay

The levels of IL-1β (CSB-E08054m), IL-18 (CSB-E04609m) in muscle tissue homogenates and ghrelin (CSB-E09817m) plasmatic levels were detected using mouse cytokine enzyme-linked immune sorbent assay (ELISA) kits (CUSABIO, Wuhan, China). The experiments were administrated according to manufacturer's instructions and each sample was analyzed in duplicate. Optical density of every well was measured at 450 nm within 5 min.

2.11. Statistical analysis

Data were analyzed with SPSS 16.0 software (SPSS, Chicago, IL, USA) and presented as means ± standard error of the mean (SEM). Two-tailed unpaired *t*-test, one way analysis of variance (ANOVA) following post hoc tests was employed for statistical analysis. Comparative differences were considered significant at $P < 0.05$.

3. Results

3.1. Ghrelin ameliorated skeletal muscle function in mdx mice

To assess the functional contribution of ghrelin in dystrophin-deficient *mdx* mice, we firstly investigated the effect of ghrelin on muscular function of *mdx* mice. We measured the endogenous ghrelin level and *mdx* mice did not show any difference in ghrelin circulating concentrations compared with wild-type mice (Supplemental Table 1). At the age of 4 weeks, *mdx* mice were treated with ghrelin or saline (Fig. 1A). After 4 weeks injection, we examined the body weight of mice in the four groups including saline-treated wild-type C57BL/10 mice, ghrelin-treated wild-type C57BL/10 mice, ghrelin-treated *mdx* mice and saline-treated *mdx* mice. In comparison to saline-treated controls, ghrelin-treated *mdx* mice showed no obvious difference in body weight (data not shown). Then, the forelimb grip strength was performed to assess the effect of ghrelin on skeletal muscle performance of *mdx* mice, which was calculated as the ratio of the grip strength to body weight.

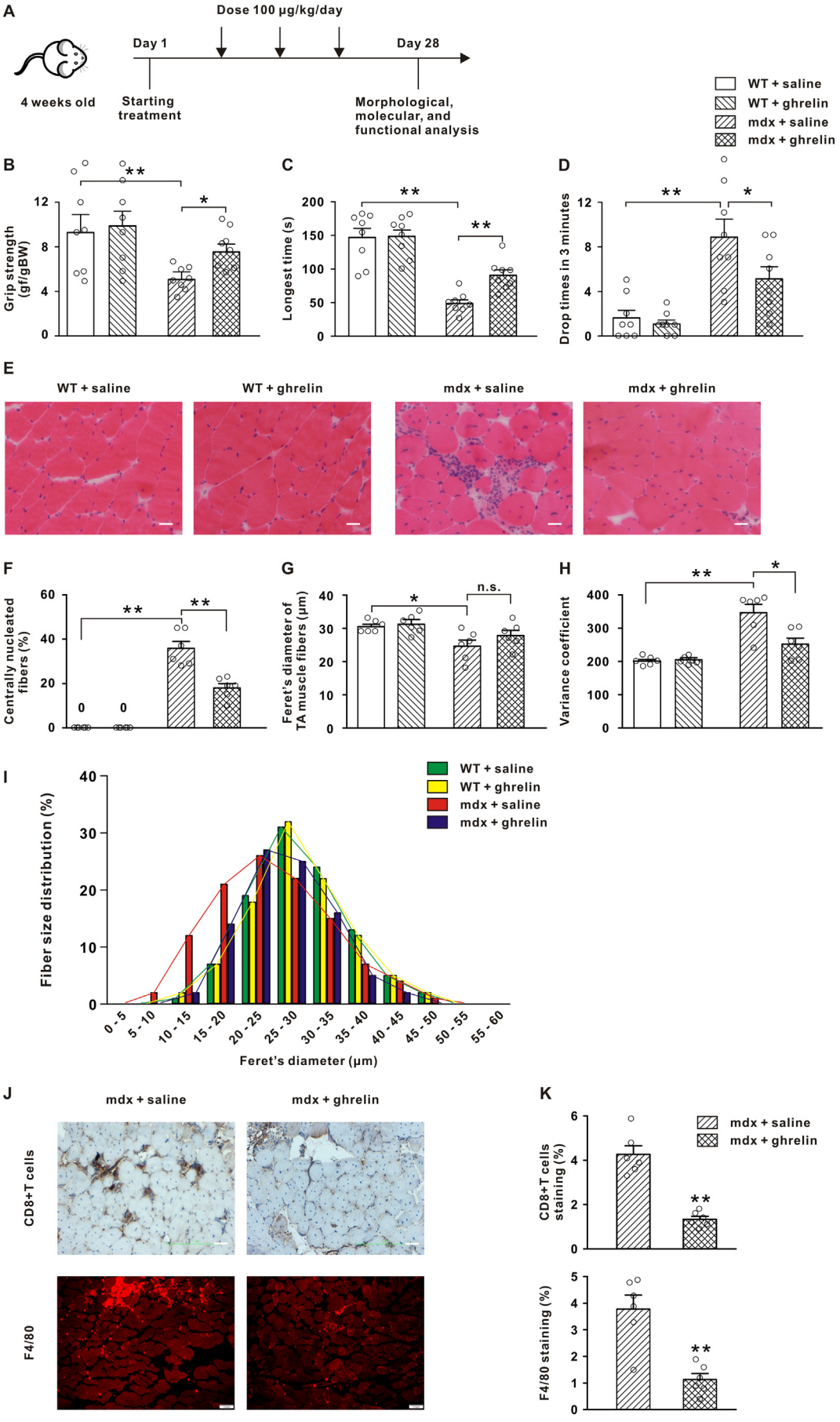

(caption on next page)

Fig. 1. Ghrelin alleviated muscle function and histopathological changes of dystrophic muscles in *mdx* mice. (A) Schematic diagram of ghrelin administration protocol in 4-week-old male *mdx* mice. *Mdx* mice were treated with ghrelin at the dose of 100 μg/kg of body weight every day and then muscle functional analysis was conducted after 28 days of injection. (B) Grip strength was examined using a grip strength meter apparatus. The result was presented as the ratio of gram-force to body weight. $n = 8$ mice per group. (C–D) The longest time on the string (C) and drop times in 3 min (D) were detected by a wire suspension test. n = 8 mice per group. (E) Morphological features of skeletal muscles from saline-treated and ghrelin-treated wild-type C57BL/10 mice (WT), ghrelin-treated *mdx* mice and saline-treated *mdx* mice were assessed on H&E staining and images of tibialis anterior muscle sections were shown(Scale bars = 50 μm). (F–H) The percentage of centrally nucleated fibers (F), minimum Feret's diameter of all fibers (G), and variance coefficient of muscle fiber size (H) were analyzed within muscle fibers from five squares randomly chosen using Image J software. Variance coefficient = (standard deviation of the muscle fiber size/mean muscle fiber size) × 1000. (**I**) Fiber size distribution in tibialis anterior muscles from saline-treated WT, ghrelin-treated WT, saline-treated *mdx* mice and ghrelin-treated *mdx* mice. (J) Muscle sections were immunostained with CD8 antibody for $CD8^+$T cells and F4/80 antibody to identify macrophages. Immunostaining images from tibialis anterior sections were presented (scale bars = 50 μm). (K) The percentage of $CD8^+$ T cells and F4/80 in different muscles of above three groups were quantified by using Image J software. The data were presented as means ± SEM. * $P < 0.05$, ** $P < 0.01$, and n.s. indicates non-significant.

The grip strength and the longest time on the string of *mdx* control mice were significantly decreased as compared to that of wild-type C57BL/10 mice (Fig. 1B-C). Meanwhile, *mdx* mice showed an obvious rise in the drop times within 3 min from the string (Fig. 1D). Noticeably, the grip strength was greatly elevated in *mdx* mice receiving ghrelin treatment, which amounted to increases of 48.4% over *mdx* values (Fig. 1B). Also, administration of ghrelin could remarkably increase the time of holding onto the string in wire suspension tests (Fig. 1C), and reduce the drop times within 3 min from the string compared with *mdx* control mice (Fig. 1D). However, ghrelin treatment did not change muscular function in wild-type mice (Fig. 1B-D). Therefore, our results indicated that ghrelin treatment improved the muscular function in *mdx* mice.

3.2. Ghrelin improved skeletal muscle pathology and decreased inflammatory cell infiltration in mdx mice

Given that ghrelin could improve muscular function of *mdx* mice, we further analyzed whether ghrelin affected the histopathological changes and inflammation cell infiltration in dystrophic muscles. We separated the mass of the limb muscles of mice in the four groups, and then frozen sections of skeletal muscles were stained with hematoxylin/eosin or immunostained with antibodies. As exhibited in Fig. 1E, the limb muscles of *mdx* control mice showed the representative histopathological changes of abnormal dystrophic muscles, including necrotic fibers, fiber hypertrophy, fibers with centrally located nuclei and inflammatory infiltration. These results revealed that *mdx* mice showed a higher proportion of muscle fibers with centralized nuclei than C57BL/10 mice, whereas ghrelin significantly decreased the percentage of centrally nucleated fibers by 49.8% compared with that of *mdx* mice (Fig. 1F). Feret's diameter of all muscle fibers within the tibialis anterior muscle was smaller in the *mdx* mice group than WT mice (Fig. 1G). Moreover, the mean coefficient of variance, which is used as an indicator of the myofiber size variability, was remarkably increased in muscle tissues (tibialis anterior) of *mdx* mice, while ghrelin-treated *mdx* mice muscles exhibited a decrease in the coefficient of variance (Fig. 1H). In addition, a fiber size distribution analysis indicated that *mdx* mice tibialis anterior muscles were presented with more proportion of small and large size myofibers in comparison with WT mice muscles, and showed a shift toward large size fibers in ghrelin-treated *mdx* mice (Fig. 1I). Consistent with the results from above muscular function, there was no difference in histological analysis between ghrelin-treated and saline-treated wild-type mice (Fig. 1E-I).

It is generally agreed upon that T lymphocytes and macrophages that are the main immune cells infiltrated within dystrophic muscles at the acute stage, play a central role in the pathogenesis of muscular dystrophy [4,8]. In comparison with *mdx* mice, ghrelin-treated *mdx* mice showed a significant reduction in the percentage of infiltrating $CD8^+$ T cells, which were identified by positive staining for CD8 on skeletal muscle sections (Fig. 1J, K). Moreover, F4/80 immunofluorescence for detecting macrophages, showed that ghrelin treatment reduced the percent of macrophages infiltration by 70% in limb muscles compared to *mdx* control mice (Fig. 1J, K). Accordingly, these results illustrated that ghrelin could improve muscle pathology and ameliorate muscle inflammation in *mdx* mice.

NLRP3 inflammasome was activated and ghrelin suppressed the NLRP3 inflammasome activation in the limb muscles of dystrophin-deficient *mdx* mice.

Considering the role of NLRP3 inflammasome in innate immune response , we next assessed whether NLRP3 inflammasome was activated in *mdx* mice and explored the underling mechanism for ghrelin-mediated inhibition of muscle inflammation. In comparison to C57BL/10 mice, NLRP3 protein expression was increased in muscle tissues of *mdx* mice (Fig. 2A). In a similar fashion, augmented ASC, pro-caspase-1, pro-IL-1β, and mature IL-1β protein expressions were observed in *mdx* mice muscles (Fig. 2A). Our data also showed that the mRNA levels of NLRP3, ASC, caspase-1 and IL-1β were significantly up-regulated in skeletal muscles from *mdx* mice compared with that in C57BL/10 control mice (Fig. 2B). Moreover, the concentrations of IL-1β and IL-18 in the muscles homogenates of *mdx* mice were also significantly elevated than those in the controls (Fig. 2C).

To further clarify the role of NLRP3 inflammasome in *mdx* mice, NLRP3 shRNA were used to knockdown NLRP3 expression. After injection of NLRP3 shRNA or scrambled shRNA, strong green fluorescence was detected in skeletal muscles using a confocal microscopy, which indicated successful transfection of shRNA - both scrambled control and shNLRP3 (Fig. 3A). As shown in Fig. 3A, B, shRNA delivery successfully and significantly decreased NLRP3 protein expression by 56.7% compared with *mdx* control mice. More importantly, NLRP3 shRNA significantly inhibited NLRP3 inflammasome activation, as evidenced by a decrease in ASC, pro-caspase-1, pro-IL-1β and IL-1β protein expressions in *mdx* muscles (Fig. 3D). In addition, NLRP3 shRNA-treated *mdx* mice showed downregulated mRNA levels of NLRP3, caspase-1 and IL-1β (Fig. 3C, E), as well as diminished concentrations of IL-1β and IL-18 in muscle homogenates (Fig. 3F, G) in comparison with scrambled shRNA-treated *mdx* mice.

As exhibited in Fig. 4A, in contrast to scrambled shRNA-treated *mdx* mice, NLRP3 shRNA treatment remarkably ameliorated histopathological changes of dystrophic muscle, as indicated by a significantly reduction in the percentage of centrally nucleated fibers (Fig. 4B), increased muscle fiber size (minimum Feret's diameter) in all kinds of fibers sampled within the *mdx* muscles (tibialis anterior) (Fig. 4C), and decrease in the mean variance coefficient (Fig. 4D). In addition, the total area of muscle sections presenting CD8 and F4/80 positivity were significantly smaller in NLRP3 shRNA-treated *mdx* mice than *mdx* control mice, amounting to decreases of 71.3% and 70.4%, respectively (Fig. 4E, F). Furthermore, downregulation of NLRP3 significantly ameliorated muscular function in *mdx* mice including the grip strength, the time of holding onto the string and the drop times within 3 min (Fig. 4G-I). Collectively, these results demonstrated that NLRP3 inflammasome played a major role in the muscular pathology and downregulation of NLRP3 can protect *mdx* muscles.

Based on the above results, we further evaluated whether ghrelin could inhibit NLRP3 inflammasome activation. In contrast to *mdx* control mice, ghrelin-treated *mdx* muscles demonstrated a 56.3% decrease in NLRP3 expression and a 55.2% reduction in IL-1β expression,

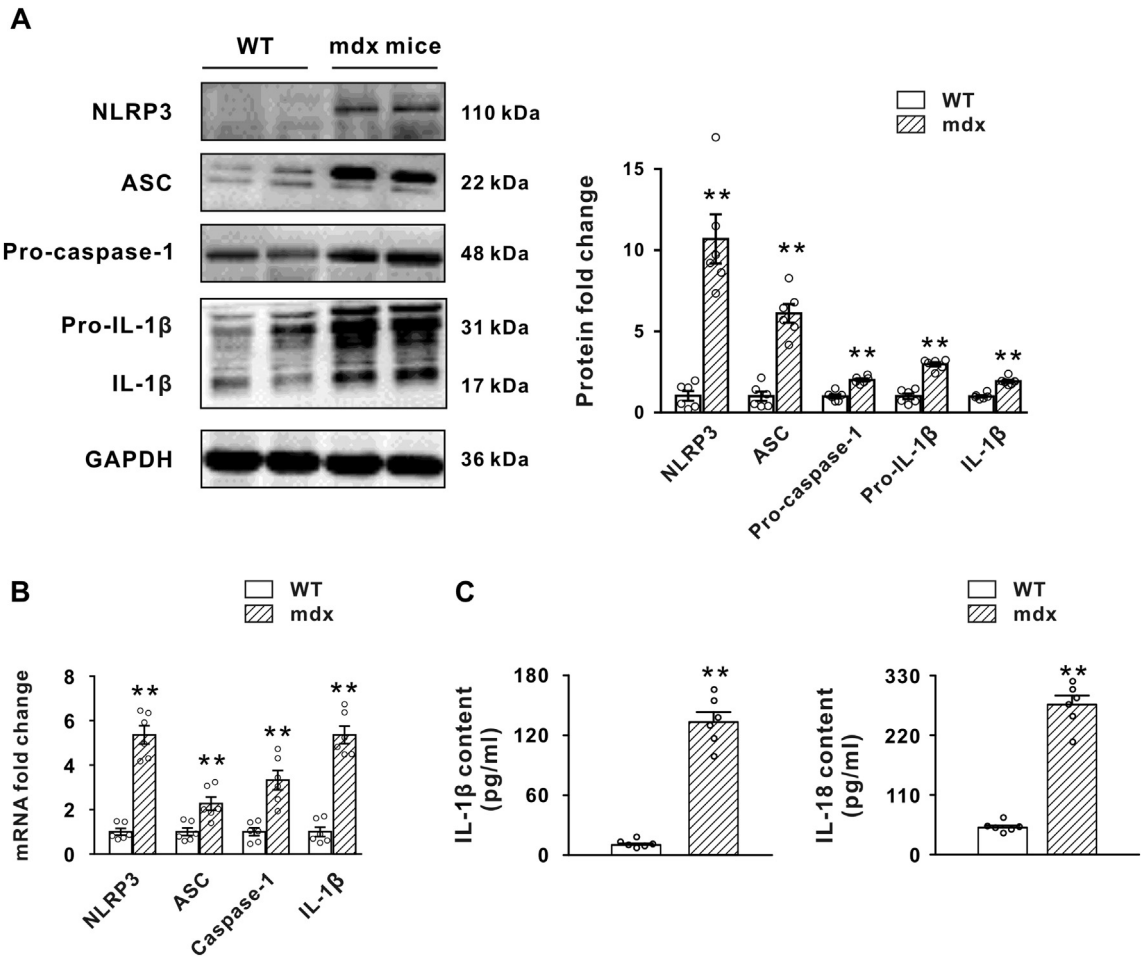

Fig. 2. NLRP3 inflammasome activation in the skeletal muscles of *mdx* mice. (**A**) Relative protein expressions of NLRP3, ASC, pro-caspase-1, pro-IL-1β and mature IL-1β in the skeletal muscles from wild-type C57BL/10 mice (WT) and *mdx* mice were determined by western blot analysis ($n = 6$ per group). The blots were quantified using the Image J software. GAPDH was used as a loading control. (**B**) Relative expression levels of NLRP3, ASC, caspase-1 and IL-1β mRNA were assessed by qRT-PCR (n = 6 per group). Values are expressed as fold change normalized to β-actin. (**C**) The concentrations of IL-1β and IL-18 in the skeletal muscle homogenates were measured by enzyme-linked immune sorbent assay (ELISA) (n = 6 per group). The data were presented as mean ± SEM, $^{*}p < 0.05$, $^{**}P < 0.01$ and n.s. indicates non-significant.

as well as a significant decrease in the protein expressions of ASC, pro-caspase-1, and pro-IL-1β (Fig. 5A). Likewise, qRT-PCR suggested that ghrelin notably reduced the mRNA levels of NLRP3, caspase-1 and IL-1β in *mdx* muscles (Fig. 5B). Furthermore, ELISA analysis also showed that both the level of IL-1β and IL-18 were significantly downregulated in muscle homogenates from ghrelin-treated group compared with the *mdx* controls (Fig. 5C). Therefore, our findings revealed that ghrelin could significantly prevent NLRP3 inflammasome activation and IL-1β secretion in dystrophic muscles.

3.3. Ghrelin inhibited NLRP3 inflammasome-mediated IL-1β production in primary myoblasts

To further identify the role of ghrelin on NLRP3 inflammasome activation including caspase-1 cleavage and IL-1β secretion, we next examined whether ghrelin could influence on the NLRP3 inflammasome activation and IL-1β secretion in vitro. We first treated LPS-primed primary myoblasts with ghrelin for 1 h, and then stimulated them with the NLRP3 inflammasome activator, the P2X7 receptor agonist benzylated ATP (BzATP). Western blot analysis exhibited that significant increases of NLRP3 (3-fold) and pro-caspase-1(2-fold) protein expression were observed in dystrophin-deficient myoblasts activated by LPS and BzATP, whereas ghrelin characteristically diminished the protein expression of NLRP3 and pro-caspase-1 by 52.0%, 48.4%, respectively (Fig. 6A). Also, ghrelin reduced the level of cleaved caspase-1 (Fig. 6A). Similar results were observed in the level of IL-1β and IL-18 from the culture supernatants. Furthermore, ghrelin significantly inhibited the secretion of IL-1β and IL-18, which was confirmed by ELISA analysis in the cell culture supernatant (Fig. 6B, C). However, there was no significant change in the IL-1β and IL-18 level in response to LPS compared to sham group (Fig. 6B, C). Collectively, these results indicated that ghrelin could inhibit IL-1β maturation and secretion by suppressing NLRP3 inflammasome activation.

3.4. Ghrelin inhibited JAK2-STAT3 and p38 MAPK signaling pathway

To explore the possible molecular mechanism for inhibition of NLRP3 inflammasome activation by ghrelin in *mdx* mice, we detected the effect of ghrelin on JAK2-STAT3, p38MAPK and JNK pathway. The Janus kinase-signal transducers and activators of transcription (JAK-STATs) and mitogen-activated protein kinases (MAPKs) signaling pathway are involved in the regulation of hematopoiesis, inflammation, immunity, cell growth, proliferation and differentiation. Western blot analysis exhibited that the level of JAK2, p-STAT3 was evidently decreased in ghrelin-treated group compared with that in *mdx* control mice (Fig. 7A, B, E). However, the level of p-JAK2 and STAT3 did not significantly change following ghrelin treatment (Fig. 7A, C, D). Moreover, we assessed the effect of ghrelin on JNK and p38MAPK

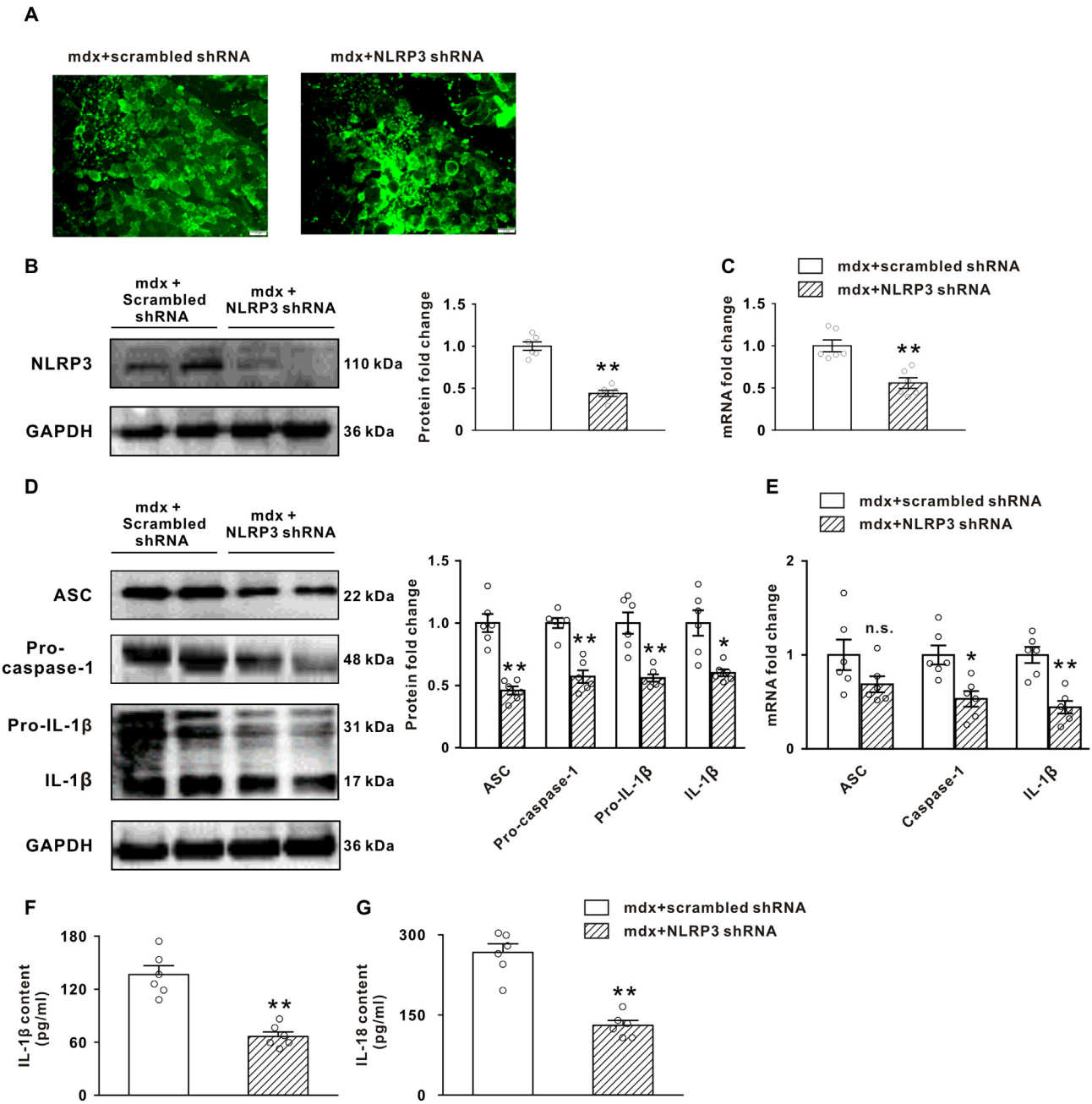

Fig. 3. NLRP3 deficiency inhibited NLRP3 inflammasome activation and diminished IL-1β and IL-18 levels in dystrophic muscles. (**A**) Representative fluorescent images of skeletal muscle sections from *mdx* mice 30d after intramuscular NLRP3 shRNA injection or scrambled shRNA. (**B**) Western blot analysis was performed to analyze the protein levels of NLRP3 in different groups of *mdx* muscles (n = 6 per group). Each lane represented a separate animal. (**C**) Quantification for the mRNA levels of NLRP3 was obtained by qRT-PCR (n = 6 per group). Values are expressed as fold change relative to β-actin. (**D**) Western blot analysis of the protein levels of ASC, pro-caspase-1, pro-IL-1β and IL-1β. The quantification for each lane was normalized to GAPDH using Image J software. Each lane represented a separate animal. (**E**) Quantification for the mRNA levels of ASC, caspase-1 and IL-1β. (**F, G**) The contents of IL-1β (F) and IL-18 (G) in *mdx* muscles receiving NLRP3 shRNA or not were examined by ELISA (n = 6 per group). * $P < 0.05$, ** $P < 0.01$ and n.s. indicates non-significant.

expression in *mdx* mice muscles. As shown in Fig. 7A, F-I, *mdx* mice receiving ghrelin treatment indicated that p-p38MAPK expression was markedly reduced, whereas the level of p38MAPK, JNK and p-JNK remained unchanged compared with saline-treated *mdx* mice. In summary, our data suggested that ghrelin inhibited NLRP3 inflammasome activation partially via JAK2-STAT3 and p38MAPK signaling pathway.

4. Discussion

Recently, many researches have demonstrated that regulating the immune response can prolong the progression of muscular dystrophy and provide an alternative intervention for treating DMD. In this study, we showed that ghrelin attenuated inflammatory recruitment to dystrophin-deficient skeletal muscle and increased centrally nucleated fibers in *mdx* mice muscles. In addition, ghrelin increased the forelimb grip strength and lengthened the times of holding onto the string in wire tests. Importantly, ghrelin inhibited the NLRP3 inflammasome activation and induced a major decrease of IL-1β and IL-18 secretion both in dystrophic muscles and primary myoblasts stimulated by LPS and the NLRP3 inflammasome activator BzATP. Taken together, above the findings revealed that ghrelin remarkably alleviated muscular phenotype and improved muscle function in *mdx* mouse model through

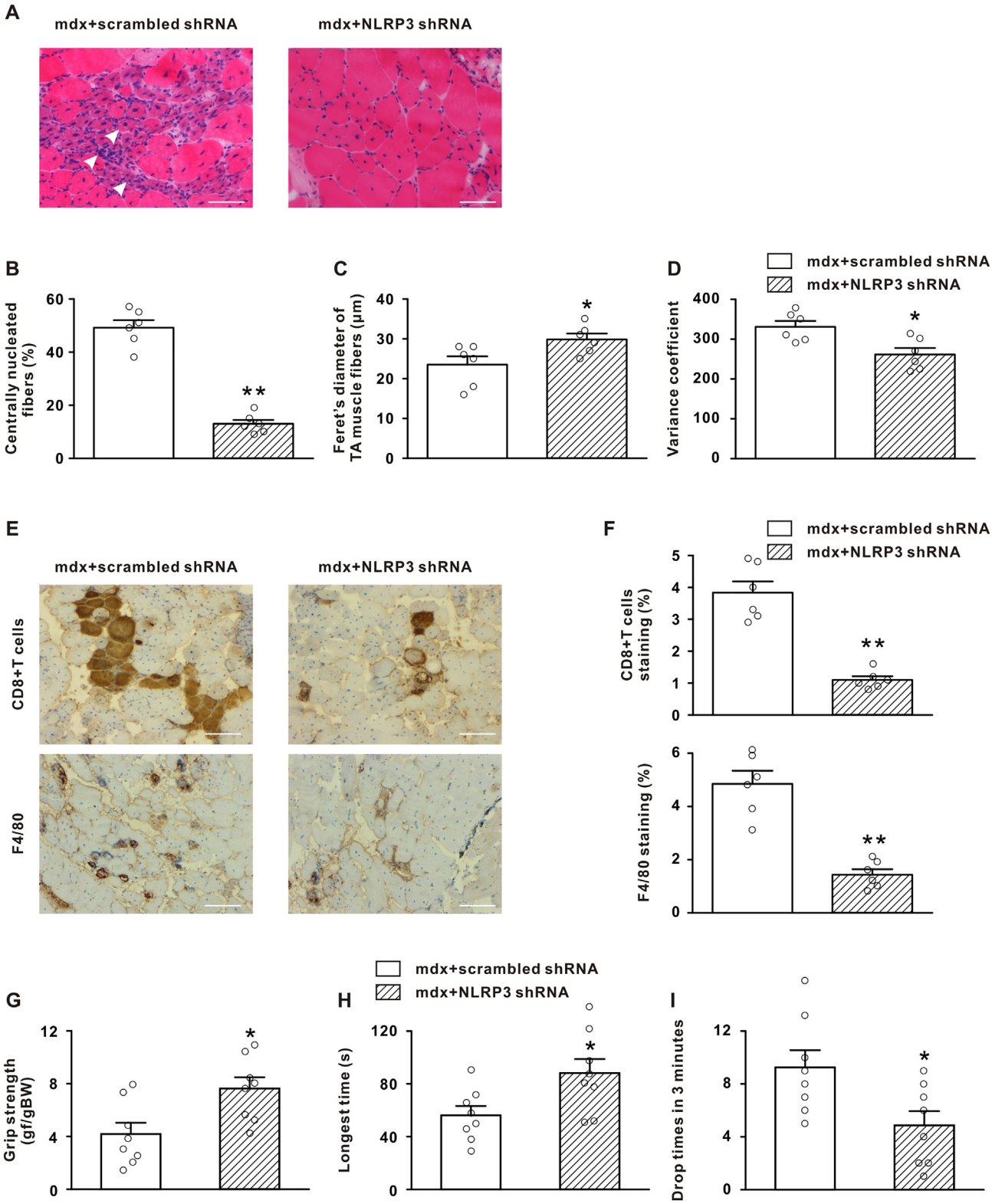

Fig. 4. NLRP3 ablation reduced dystrophic muscle pathology and improved muscle function in *mdx* mice. (**A**) Images of hematoxylin and eosin stained muscle sections of tibialis anterior muscle from NLRP3 shRNA-treated mice and scrambled shRNA-treated mice; scale bars = 50 μm. Muscle fibers with centralized nuclei, inflammatory cell infiltration and necrotic lesions were indicated by arrowhead. (B–D) The percentage of centrally nucleated fibers (B), Minimum Feret's diameter of all tibialis anterior fibers (C) and variance coefficient of muscle fiber size (D) were quantified in five squares randomly chosen using Image J software. (**E**) Immunohistochemical images of $CD8^+$ T lymphocyte or F4/80 staining in tibialis anterior muscle of mice; scale bars = 50 μm. (**F**) The total area of muscle sections presenting CD8 and F4/80 positivity in different muscles of *mdx* mice after NLRP3 shRNA or scrambled shRNA intervention were measured using Image J software. Data shown represented three independent experiments, n = 6 mice per group. (**G**) Grip strength was measured by a computerized grip strength meter apparatus (n = 8 per group). The forelimb muscle force was expressed in gram-force relative to body weight. (H, I) The longest time on the string (H) and drop times in 3 min (I) were assessed by a wire suspension test (n = 8 per group). * $P < 0.05$, ** $P < 0.01$.

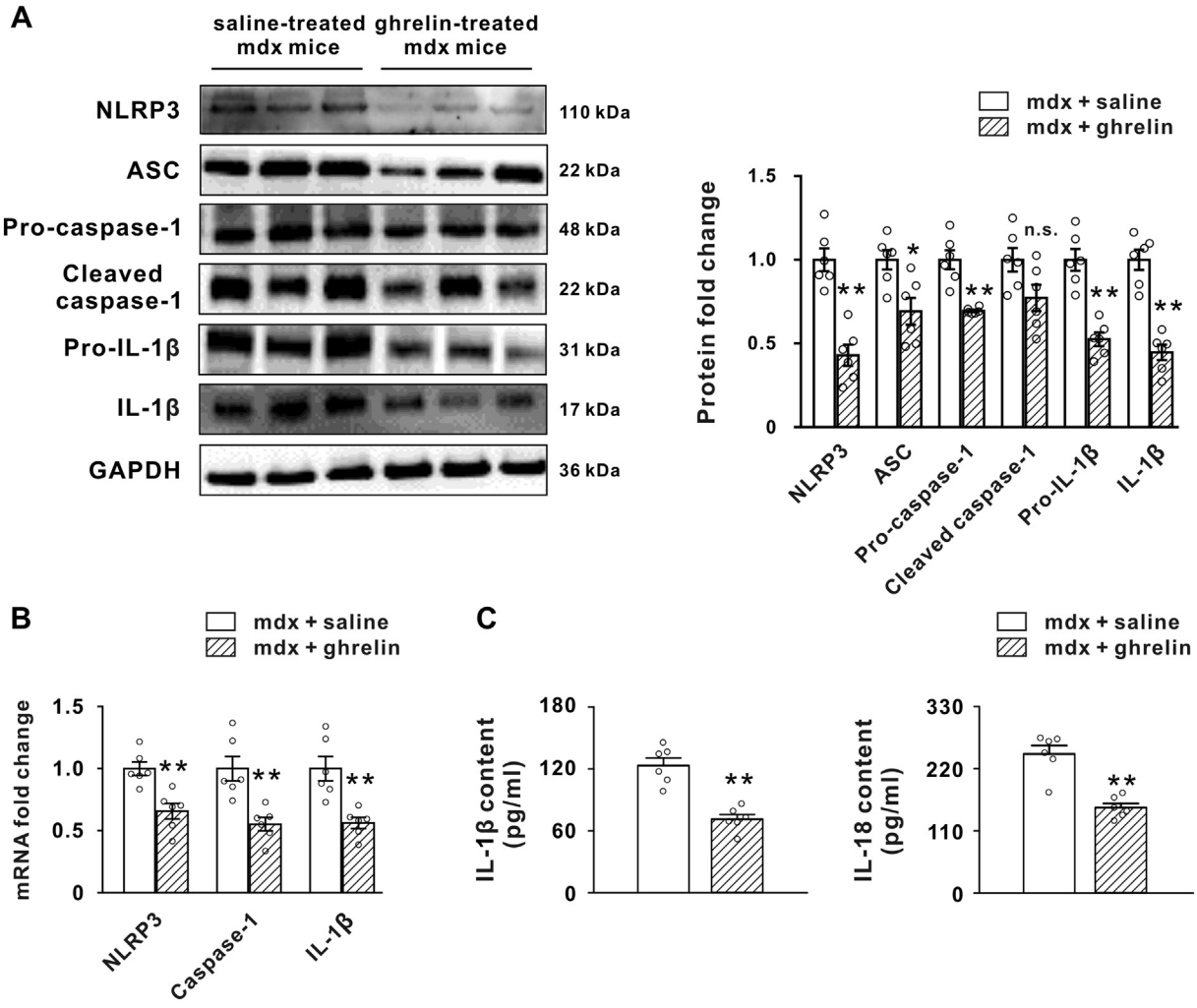

Fig. 5. Ghrelin suppressed NLRP3 inflammasome activation in *mdx* mice muscles. (**A**) Protein expressions of NLRP3, ASC, pro-caspase-1, cleaved caspase-1, pro-IL-1β and IL-1β in the muscles of *mdx* mice following treatment with ghrelin or vehicle. Quantification of above protein expression was performed by using Image J software. GAPDH severed as a loading control. (**B**) qRT-PCR analysis of NLRP3, caspase-1 and IL-1β in the skeletal muscles. (**C**) The level of IL-1β and IL-18 in muscle homogenates were detected by ELISA analysis. All data are the means ± SEM. n = 6 mice per group. * $P < 0.05$, ** $P < 0.01$, and n.s. indicates non-significant.

inhibition of the NLRP3 inflammasome activation, indicating that ghrelin exhibited considerate therapeutic benefits to *mdx* mice and may be effective in treatment of muscular dystrophy.

In the present study, we evaluated the effect of ghrelin on disease phenotype in Duchenne muscular dystrophy mouse model. It is generally agreed upon that the *mdx* mouse remains an appropriate model for pre-clinical studies [29,30]. In agreement with previous studies [2,5,6], we and others have shown that histopathological analysis of *mdx* mice muscle sections presented with inflammation infiltration, necrotic lesions, phagocytosis and muscle fibers with centrally located nuclei in limb muscles. Remarkably, our results also revealed that ghrelin significantly reduced muscle inflammation and attenuated muscle pathology in *mdx* mice. An obvious improvement of muscle morphological parameters was observed after treatment of *mdx* mice with ghrelin, as evidenced by reduced inflammatory cell infiltrate ($CD8^+$T cells and macrophages), decreased percentage of centrally nucleated fibers and reduced in the mean variance coefficient. Spencer et al. have reported that there was a 61% reduction in muscle histopathology after $CD4^+$ T cell depletion and a 75% reduction after $CD8^+$ T cell depletion in *mdx* mice [4]. In our study, we also performed immunostaining of $CD4^+$T lymphocytes on randomly selected muscle sections and found no significant difference in $CD4^+$T lymphocytes infiltration between saline-treated *mdx* mice and ghrelin-treated *mdx* mice (data not shown). In addition, we measured body weights of mice in all groups before and after interventions. Our results demonstrated that *mdx* mice showed a lighter body weight than the wild-type C57BL/10 mice. After treating *mdx* mice with ghrelin, the body weights of *mdx* mice were slightly increased and showed no significant difference between ghrelin-treated *mdx* mice and saline-treated *mdx* control mice. Noticeably, ghrelin improved muscle strength and function: ghrelin-treated *mdx* mice were stronger than *mdx* control mice in regard to the forelimb grip strength. Likewise, *mdx* mice receiving ghrelin treatment were able to hang 1.9 times longer than *mdx* control mice in wire suspension tests. These findings confirm that ghrelin confers substantial therapeutic benefits to *mdx* mice through interfering with muscle inflammation and muscle pathology. We also assessed whether down-regulation of ghrelin affected muscular function of *mdx* mice and found no significant difference in muscular function between ghrelin shRNA-treated and scrambled shRNA-treated *mdx* mice (Supplemental Fig. 1).

It has been shown that IL-1β plays a role in muscle pathology of DMD patients and primary muscle cells from *mdx* mice produce great amounts of IL-1β, which is involved in initiation and persistence of muscle inflammation [26]. Likewise, suppression of IL-1β pathway can improve muscle function in *mdx* mice [31]. Active, the NLRP3 inflammasome is crucial for synthesis and secretion of mature IL-1β, which is activated by several signals including tissue damage and endogenous danger signals [18]. It has been well established that two signals are required for the NLRP3 inflammasome activation. First, TLR

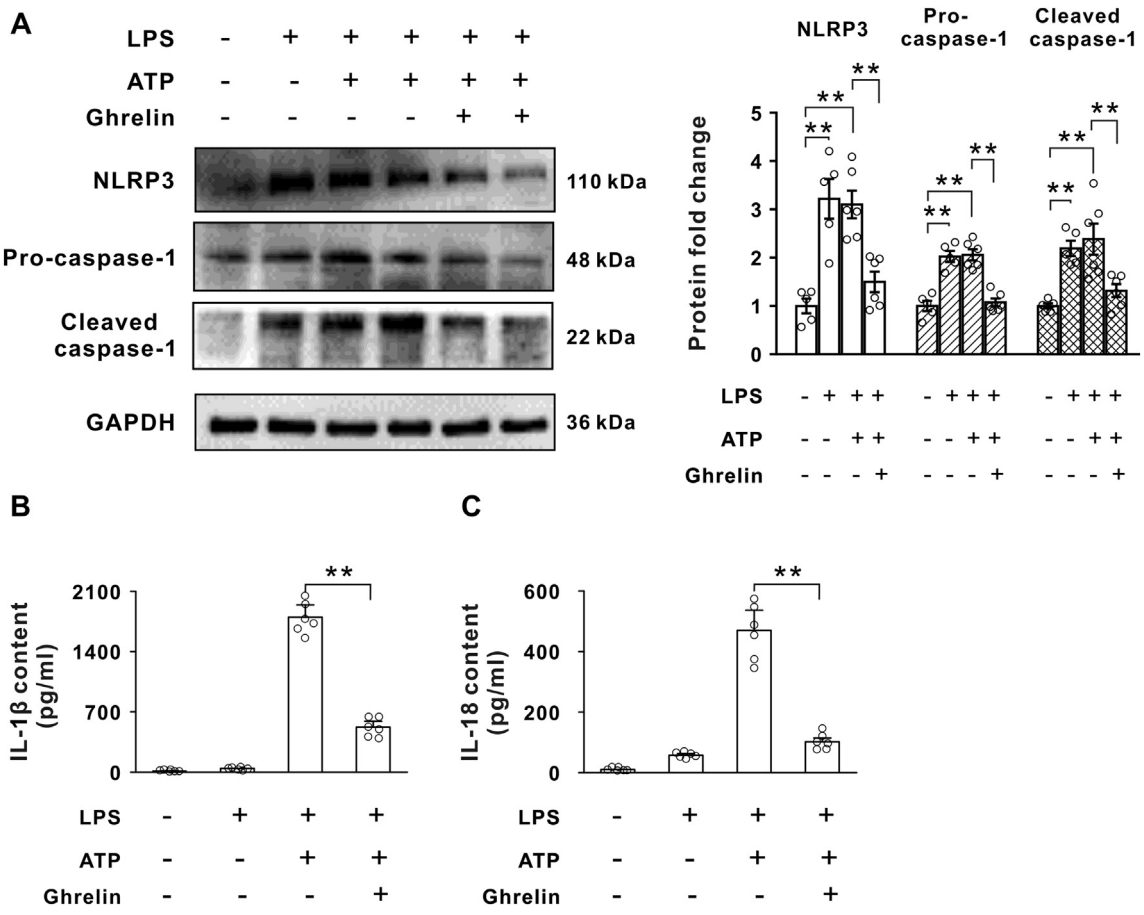

Fig. 6. Ghrelin inhibited the NLRP3 inflammasome aviation and IL-1β secretion in primary myoblasts. (**A**) LPS-primed primary myoblasts with ghrelin for 1 h and then treated them with benzylated ATP (BzATP). Protein expression were analyzed for NLRP3, pro-caspase-1 and cleaved caspase-1 by Western blot from cell extracts. Quantification of each lane was analyzed using Image J software. GAPDH severed as a loading control. (B, C) ELISA analysis was performed to detect the level of IL-1β (B) and IL-18 (C) in medium supernatants. All results were presented as the means ± SEM. n = 6 mice per group. * $P < 0.05$, ** $P < 0.01$ and n.s. indicates non-significant.

agonist (such as lipopolysaccharide, LPS) trigger the generation of pro-IL-1β and NLRP3 through the activation of NF-κB pathway (priming phase). Second, various stimuli (such as ATP, nigericin, MSU and aluminum crystals) are necessary for NLRP3 inflammasome assembling, activation of caspase-1 and the subsequent secretion of mature IL-1β [18–21]. And, caspase-1 activation which leads to cleavage of pro-caspase-1 into active caspase-1, is essential for the production and secretion of IL-1β and IL-18. It has been believed that the NLRP3 inflammasome plays a major role in regulating the immune response and participates in several inflammatory diseases [21]. Similarly, in primary myoblasts model, muscle cells have been demonstrated to be involved in inflammasome formation [26]. In this study, the increased expression of the NLRP3 inflammasome observed in the muscle from dystrophin-deficient *mdx* mice is consistent with the previous investigation [22,26]. Here, we observed that NLRP3 and caspase-1 were required for the activation of IL-1β in *mdx* mice. In addition, NLRP3 deficiency reduced the level of IL-1β and alleviated muscle pathology in *mdx* mice muscles. Moreover, Boursereau et al. [22] have found that NLRP3 expression is substantially elevated not only within dystrophic muscles of *mdx* mice but also in primary cultures of human myotubes [22]. Consequently, NLRP3 inhibitors may be available for a novel therapy in DMD.

Another intriguing finding of our study was that ghrelin could inhibit the NLRP3 inflammasome activation and mature IL-1β production. We found that the NLRP3 inflammasome was activated in dystrophic muscle, whereas ghrelin treatment evidently reduced expression of NLRP3 inflammasome components and mature IL-1β. Furthermore, our results indicated that NLRP3 and IL-1β expression were markedly raised in primary myoblasts induced by LPS and ATP in vitro. Also, we confirmed that ghrelin could suppress NLRP3 inflammasome activation and IL-1β secretion by stimuli ATP. In brief, these results demonstrated that ghrelin exerted anti-inflammatory property in *mdx* mice through inhibition of NLRP3 inflammasome activation.

Furthermore, our results indicated that anti-inflammatory effect of ghrelin may be mediated in part by down-regulation of JAK2-STAT3 and p38 MAPK pathway. Our study showed that JAK2-STAT3 signaling pathway was strongly decreased in ghrelin-treated group compared with saline-treated group. Reportedly, the JAK-STAT pathway plays an important role in inflammation, immunity and immune-related diseases [32,33]. This study suggested that JAK2 and the phosphorylation of STAT3 were decreased in dystrophic muscles receiving ghrelin treatment, while the phosphorylation of JAK2 presented no obvious change, which indicated that ghrelin may only affected the level of tyrosine kinases. Additional signal pathway is currently being investigated. Additionally, it is generally accepted that mitogen-activated protein kinases (MAPK) pathway plays important roles in regulating inflammatory responses [34]. Previous study has revealed that ghrelin could inhibit apoptosis of cardiomyocytes via activation of ERK1/2 and PI 3-kinase/AKT pathways [35]. Similarly, ghrelin inhibits hydrogen peroxide-induced apoptotic cell death of oligodendrocytes via ERK and p38MAPK signaling [36]. In the present study, we found that ghrelin down-regulated p38MAPK phosphorylation in *mdx* muscles. Moreover, it has been reported that the MAPK pathway is involved in mediating

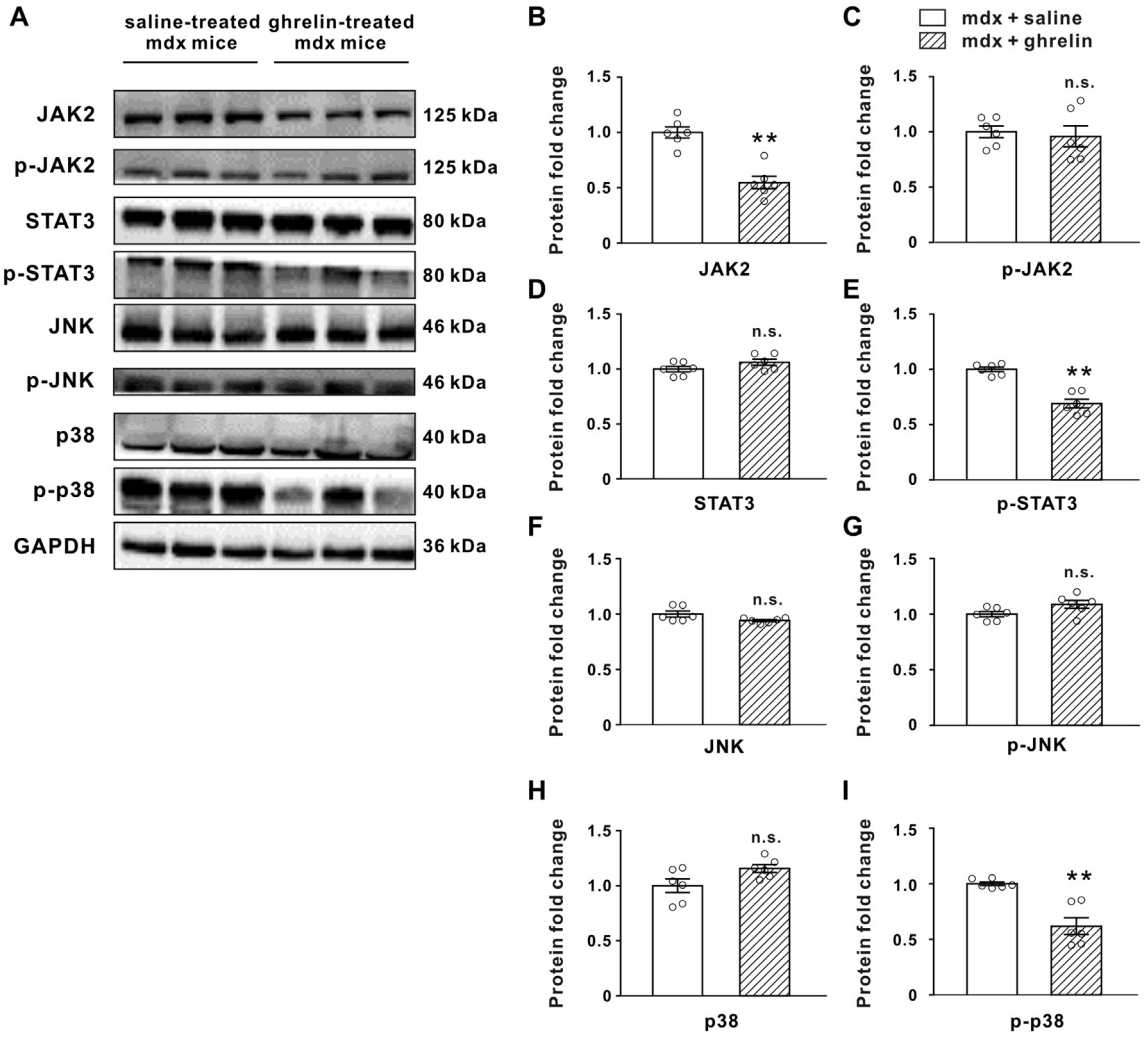

Fig. 7. Ghrelin inhibited JAK2-STAT3 and p38 MAPK signaling pathway. (A) The protein expressions of JAK2, p-JAK2, STAT3, p-STAT3, JNK, p-JNK, p38 and p-p38 were detected by western blot analysis. (B–I) The relative intensity of the bands was quantitated in JAK2 (B), p-JAK2 (C), STAT3 (D), p-STAT3 (E), JNK (F), p-JNK (G), p38 (H) and p-p38 (I) by using Image J software. GAPDH was used as a loading control. Above results were obtained from three independent experiments. The data were presented as means ± SEM. * $P < 0.05$, ** $P < 0.01$ and n.s. indicates non-significant.

NLRP3 inflammasome activation, thus reflecting that ghrelin may inhibit NLRP3 inflammasome activation partly by suppressing p38MAPK phosphorylation. This study has certain limitations. Since genetic drift may affect experimental results, it would have been more appropriate for the experimental design to use wildtype littermate controls.

5. Conclusions

In summary, our results demonstrate that ghrelin not only reduces inflammatory infiltration within dystrophin-deficient muscles, but also improves muscle morphological change in *mdx* mice. Moreover, our results further show that ghrelin significantly reduces IL-1β secretion in primary myoblast through suppression of the NLRP3 inflammasome. Furthermore, ghrelin may prevent NLRP3 inflammasome activation partly via JAK2-STAT3 and p38 MAPK pathway in *mdx* muscles. Therefore, our study offers an anti-inflammatory therapy and strong evidence to support the therapeutic potential of ghrelin for DMD.

Authors' contributions

YX designed the experiments and wrote the manuscript. LC performed the animal experiments, cell culture and molecular biological experiments and interpreted the results. FN conducted behavioral tests, performed the staining and analyzed the results. JC, XC, ZL and YB performed the staining, cell culture and molecular biological experiments. LC prepared figures and drafts. All authors read and approved the final manuscript.

Ethics approval

The animal study protocols were approved by the Experimental Animal Care and Use Committee of Nanjing Medical University. The experiments were operated according to the guidelines for the Care and Use of Laboratory Animal provided by the US National Institutes of Health (NIH publications No. 8023, revised 1978).

Declaration of Competing Interest

The authors declare that there are no conflicts of interest.

Acknowledgments

This work was supported by the National Natural Science Foundation of China (81671113), the Key Research and Development Project of Jiangsu Province of China (BE2016610), the Project of Invigorating Health Care through Science, Technology and Education

(QNRC2016026).

Appendix A. Supplementary data

Supplementary data to this article can be found online at https://doi.org/10.1016/j.lfs.2019.116654.

References

[1] A.S. Rosenberg, M. Puig, K. Nagaraju, E.P. Hoffman, S.A. Villalta, V.A. Rao, et al., Immune-mediated pathology in Duchenne muscular dystrophy, Sci. Transl. Med. 7 (299) (2015) 299rv4, https://doi.org/10.1126/scitranslmed.aaa7322.

[2] C.-C. Sun, S.-J. Li, C.-L. Yang, R.-L. Xue, Y.-Y. Xi, L. Wang, et al., Sulforaphane attenuates muscle inflammation in dystrophin-deficient *mdx* mice via NF-E2-related factor 2 (Nrf2)-mediated inhibition of NF-κB signaling pathway, J. Biol. Chem. 290 (29) (2015) 17784–17795, https://doi.org/10.1074/jbc.M115.655019.

[3] J.D. Porter, A chronic inflammatory response dominates the skeletal muscle molecular signature in dystrophin-deficient mdx mice, Hum. Mol. Genet. 11 (3) (2002) 263–272.

[4] M.J. Spencer, E. Montecino-Rodriguez, K. Dorshkind, J.G. Tidball, Helper (CD4 +) and cytotoxic (CD8 +) T cells promote the pathology of dystrophin-deficient muscle, Clin. Immunol. 98 (2) (2001) 235–243, https://doi.org/10.1006/clim.2000.4966.

[5] C. Giordano, K. Mojumdar, F. Liang, C. Lemaire, T. Li, J. Richardson, et al., Toll-like receptor 4 ablation in mdx mice reveals innate immunity as a therapeutic target in Duchenne muscular dystrophy, Hum. Mol. Genet. 24 (8) (2015) 2147–2162, https://doi.org/10.1093/hmg/ddu735.

[6] K. Mojumdar, F. Liang, C. Giordano, C. Lemaire, G. Danialou, T. Okazaki, et al., Inflammatory monocytes promote progression of Duchenne muscular dystrophy and can be therapeutically targeted via CCR2, EMBO Mol Med 6 (11) (2014) 1476–1492, https://doi.org/10.15252/emmm.201403967.

[7] S.A. Villalta, B. Deng, C. Rinaldi, M. Wehling-Henricks, J.G. Tidball, IFN-γ promotes muscle damage in the *mdx* mouse model of Duchenne muscular dystrophy by suppressing M2 macrophage activation and inhibiting muscle cell proliferation, J. Immunol. 187 (10) (2011) 5419–5428, https://doi.org/10.4049/jimmunol.1101267.

[8] S.A. Villalta, C. Rinaldi, B. Deng, G. Liu, B. Fedor, J.G. Tidball, Interleukin-10 reduces the pathology of mdx muscular dystrophy by deactivating M1 macrophages and modulating macrophage phenotype, Hum. Mol. Genet. 20 (4) (2011) 790–805, https://doi.org/10.1093/hmg/ddq523.

[9] K. Bushby, R. Finkel, D.J. Birnkrant, L.E. Case, P.R. Clemens, L. Cripe, et al., Diagnosis and management of Duchenne muscular dystrophy, part 1: diagnosis, and pharmacological and psychosocial management, Lancet Neurol. 9 (4) (2010) 77–93, https://doi.org/10.1016/S1474-4422(09)70271-6.

[10] C.-Y. Chen, A. Asakawa, M. Fujimiya, S.-D. Lee, A. Inui, Ghrelin gene products and the regulation of food intake and gut motility, Pharmacol. Rev. 61 (4) (2009) 430–481, https://doi.org/10.1124/pr.109.001958.

[11] P.E. Porporato, N. Filigheddu, S. Reano, M. Ferrara, E. Angelino, V.F. Gnocchi, et al., Acylated and unacylated ghrelin impair skeletal muscle atrophy in mice, J. Clin. Invest. 123 (2) (2013) 611–622, https://doi.org/10.1172/JCI39920.

[12] S. Reano, E. Angelino, M. Ferrara, V. Malacarne, H. Sustova, O. Sabry, et al., Unacylated ghrelin enhances satellite cell function and relieves the dystrophic phenotype in Duchenne muscular dystrophy mdx model, Stem Cells 35 (7) (2017) 1733–1746, https://doi.org/10.1002/stem.2632.

[13] D. Baatar, K. Patel, D.D. Taub, The effects of ghrelin on inflammation and the immune system, Mol. Cell. Endocrinol. 340 (1) (2011) 44–58, https://doi.org/10.1016/j.mce.2011.04.019.

[14] C.-X. Huang, M.-J. Yuan, H. Huang, G. Wu, Y. Liu, S.-B. Yu, et al., Ghrelin inhibits post-infarct myocardial remodeling and improves cardiac function through anti-inflammation effect, Peptides 30 (12) (2009) 2286–2291, https://doi.org/10.1016/j.peptides.2009.09.004.

[15] G.-X. Sun, R. Ding, M. Li, Y. Guo, L.-P. Fan, L.-S. Yue, et al., Ghrelin attenuates renal fibrosis and inflammation of obstructive nephropathy, J. Urol. 193 (6) (2015) 2107–2115, https://doi.org/10.1016/j.juro.2014.11.098.

[16] M. Naghibosadat, T. Lalonde, L. Luyt, L. Hoffman, S. Dhanvantari, Ghrelin and des-acyl ghrelin binding in cardiac tissue are altered with cardiovascular inflammation in Duchenne muscular dystrophy, Can Cardiovasc Soc EPosters (2018) 052.

[17] N. Filigheddu, V.F. Gnocchi, M. Coscia, M. Cappelli, P.E. Porporato, R. Taulli, et al., Ghrelin and des-acyl ghrelin promote differentiation and fusion of C2C12 skeletal muscle cells, Mol. Biol. Cell 18 (3) (2007) 986–994, https://doi.org/10.1091/mbc.e06-05-0402.

[18] K. Schroder, J. Tschopp, The Inflammasomes, Cell 140 (6) (2010) 821–832, https://doi.org/10.1016/j.cell.2010.01.040.

[19] L. Franchi, T. Eigenbrod, R. Muñoz-Planillo, G. Nuñez, The inflammasome: a caspase-1-activation platform that regulates immune responses and disease pathogenesis, Nat. Immunol. 10 (3) (2009) 241–247, https://doi.org/10.1038/ni.1703.

[20] E. Latz, The inflammasomes: mechanisms of activation and function, Curr. Opin. Immunol. 22 (1) (2010) 28–33, https://doi.org/10.1016/j.coi.2009.12.004.

[21] E.-K. Jo, J.K. Kim, D.-M. Shin, C. Sasakawa, Molecular mechanisms regulating NLRP3 inflammasome activation, Cell Mol Immunol 13 (2) (2016) 148–159, https://doi.org/10.1038/cmi.2015.95.

[22] R. Boursereau, M. Abou-Samra, S. Lecompte, L. Noel, S.M. Brichard, Downregulation of the NLRP3 inflammasome by adiponectin rescues Duchenne muscular dystrophy, BMC Biol. 16 (1) (2018) 33, https://doi.org/10.1186/s12915-018-0501-z.

[23] L. Yu, Y. Liu, H. Yang, X. Zhu, X. Cao, J. Gao, et al., PSD-93 attenuates amyloid-β-mediated cognitive dysfunction by promoting the catabolism of amyloid-β, J. Alzheimers Dis. 59 (3) (2017) 913–927, https://doi.org/10.3233/JAD-170320.

[24] Y. Pan, C. Chen, Y. Shen, C.-H. Zhu, G. Wang, X.-C. Wang, et al., Curcumin alleviates dystrophic muscle pathology in mdx mice, Mol Cells 25 (4) (2008) 531–537.

[25] J. Jin, A.K.F. Liou, Y. Shi, K. Yin, L. Chen, L. Li, et al., CART treatment improves memory and synaptic structure in APP/PS1 mice, Sci. Rep. 5 (2015) 10224, , https://doi.org/10.1038/srep10224.

[26] R. Rawat, T.V. Cohen, B. Ampong, D. Francia, A. Henriques-Pons, E.P. Hoffman, et al., Inflammasome up-regulation and activation in Dysferlin-deficient skeletal muscle, Am. J. Pathol. 176 (6) (2010) 2891–2900, https://doi.org/10.2353/ajpath.2010.090058.

[27] H. Yin, Q. Guo, X. Li, T. Tang, C. Li, H. Wang, et al., Curcumin suppresses IL-1β secretion and prevents inflammation through inhibition of the NLRP3 Inflammasome, J. Immunol. 200 (8) (2018) 2835–2846, https://doi.org/10.4049/jimmunol.1701495.

[28] Y. Xu, W. Zhang, J. Klaus, J. Young, I. Koerner, L.C. Sheldahl, et al., Role of cocaine- and amphetamine-regulated transcript in estradiol-mediated neuroprotection, Proc. Natl. Acad. Sci. U. S. A. 103 (39) (2006) 14489–14494, https://doi.org/10.1073/pnas.0602932103.

[29] L. Pelosi, M.G. Berardinelli, L. De Pasquale, C. Nicoletti, A. D'Amico, F. Carvello, et al., Functional and morphological improvement of dystrophic muscle by interleukin 6 receptor blockade, EBioMedicine 2 (4) (2015) 285–293, https://doi.org/10.1016/j.ebiom.2015.02.014.

[30] S. Bogdanovich, T.O.B. Krag, E.R. Barton, L.D. Morris, L.-A. Whittemore, R.S. Ahima, et al., Functional improvement of dystrophic muscle by myostatin blockade, Nature 420 (6914) (2002) 418–421, https://doi.org/10.1038/nature01154.

[31] M.E. Benny Klimek, A. Sali, S. Rayavarapu, J.H. Van der Meulen, K. Nagaraju, Effect of the IL-1 receptor antagonist Kineret® on disease phenotype in mdx mice. Kumar a, editor, PLoS One 11 (5) (2016) e0155944, https://doi.org/10.1371/journal.pone.0155944.

[32] R.A. Eid, M.A. Alkhateeb, S. Eleawa, F.H. Al-Hashem, M. Al-Shraim, A.F. El-kott, et al., Cardioprotective effect of ghrelin against myocardial infarction-induced left ventricular injury via inhibition of SOCS3 and activation of JAK2/STAT3 signaling, Basic Res. Cardiol. 113 (2:13) (2018), https://doi.org/10.1007/s00395-018-0671-4.

[33] Y.-N. Jang, E.J. Baik, JAK-STAT pathway and myogenic differentiation, JAKSTAT 2 (2) (2013) e23282, , https://doi.org/10.4161/jkst.23282.

[34] Wang. The inhibitory effect of ghrelin on sepsis-induced inflammation is mediated by the MAPK phosphatase-1. Int. J. Mol. Med.. 2010; 25(1):159–64.

[35] G. Baldanzi, N. Filigheddu, S. Cutrupi, F. Catapano, S. Bonissoni, A. Fubini, et al., Ghrelin and des-acyl ghrelin inhibit cell death in cardiomyocytes and endothelial cells through ERK1/2 and PI 3-kinase/AKT, J. Cell Biol. 159 (6) (2002) 1029–1037, https://doi.org/10.1083/jcb.200207165.

[36] J.Y. Lee, T.H. Oh, T.Y. Yune, Ghrelin inhibits hydrogen peroxide-induced apoptotic cell death of oligodendrocytes via ERK and p38MAPK signaling, Endocrinology 152 (6) (2011) 2377–2386, https://doi.org/10.1210/en.2011-0090.